

A Noble-Metal-Free, Tetra-nickel Polyoxotungstate Catalyst for Efficient Photocatalytic Hydrogen Evolution

Hongjin Lv,[†] Weiwei Guo,[†] Kaifeng Wu,[†] Zheyuan Chen,[†] John Bacsa,[‡] Djamaladdin G. Musaev,[§] Yurii V. Geletii,[†] Sarah M. Lauinger,[†] Tianquan Lian,[†] and Craig L. Hill^{*,†}

[†]Department of Chemistry, [‡]X-ray Crystallography Center and [§]Cherry L. Emerson Center for Scientific Computation, Emory University, 1515 Dickey Drive, Atlanta, Georgia 30322, United States

S Supporting Information

ABSTRACT: A tetra-nickel-containing polyoxotungstate, $\text{Na}_6\text{K}_4[\text{Ni}_4(\text{H}_2\text{O})_2(\text{PW}_9\text{O}_{34})_2] \cdot 32\text{H}_2\text{O}$ ($\text{Na}_6\text{K}_4\text{-Ni}_4\text{P}_2$), has been synthesized in high yield and systematically characterized. The X-ray crystal structure confirms that a tetra-nickel cluster core $[\text{Ni}_4\text{O}_{14}]$ is sandwiched by two trivacant, heptadentate $[\text{PW}_9\text{O}_{34}]^{9-}$ POM ligands. When coupled with (4,4'-di-*tert*-butyl-2,2'-dipyridyl)-bis(2-phenylpyridine(1*H*))-iridium(III) hexafluorophosphate $[\text{Ir}(\text{ppy})_2(\text{dtbbpy})][\text{PF}_6]$ as photosensitizer and triethanolamine (TEOA) as sacrificial electron donor, the noble-metal-free complex Ni_4P_2 works as an efficient and robust molecular catalyst for H_2 production upon visible light irradiation. Under minimally optimized conditions, Ni_4P_2 catalyzes H_2 production over 1 week and achieves a turnover number (TON) of as high as 6500 with almost no loss in activity. Mechanistic studies (emission quenching, time-resolved fluorescence decay, and transient absorption spectroscopy) confirm that, under visible light irradiation, the excited state $[\text{Ir}(\text{ppy})_2(\text{dtbbpy})]^{+*}$ can be both oxidatively and reductively quenched by Ni_4P_2 and TEOA, respectively. Extensive stability studies (e.g., UV-vis absorption, FT-IR, mercury-poison test, dynamic light scattering (DLS) and transmission electron microscopy (TEM)) provide very strong evidence that Ni_4P_2 catalyst remains homogeneous and intact under turnover conditions.

The photocatalytic splitting of water into dihydrogen and dioxygen utilizing solar energy has become a very active research area recently.¹ Current research endeavors focus on developing efficient, robust, inexpensive, sustainable, and environmentally benign catalytic systems for each half reaction, i.e. water oxidation or water reduction. Since early reports on molecular photocatalytic water-reducing systems in the late 1970s,² many organometallic complexes of several earth-abundant metals including iron,³ cobalt,⁴ nickel,⁵ and molybdenum⁶ have been used as molecular catalysts for photochemically and electrochemically driven hydrogen production. Although some of these systems are sufficiently robust to achieve high turnover numbers (TON > 10^3),^{4c,e,f,5a,c-e} many others have the problems of either low efficiency, limited solubility in aqueous media, instability toward strong acidic environments, or they deactivate by ligand dissociation, decomposition and/or hydrogenation.⁷ Therefore,

the development of new transition-metal-based catalysts that are highly efficient, very stable, structurally and geometrically tunable remains a substantial challenge.

Polyoxometalates (POMs), a large family of transition-metal oxygen-anion clusters with d^0 electronic configurations, are attractive candidates for catalysis of multielectron processes because of their extensive tunability, rich redox chemistry and high stability toward hydrolysis in water or hydrogenation under reducing conditions.⁸ Recently, transition-metal-substituted POMs have been extensively investigated as water oxidation catalysts (WOCs) under thermal,⁹ photochemical¹⁰ and electrochemical¹¹ conditions; however, this is not the case for POM-based water reduction catalysts (WRCs). There are early studies that show reduced POMs evolve H_2 via photochemical¹² or electrochemical¹³ processes, but all these studies involve either strong UV-light irradiation or the use of Pt(0) as a cocatalyst.

To date, there are only few reports on visible-light-driven H_2 evolution by POM WRCs,¹⁴ and only two of them are Pt(0) free.^{14c,d} The first example by Artero, Izzet, and co-workers involves a covalently linked Ir(III)-photosensitized polyoxometalate complex, which catalyzes H_2 production with a TON of 41 after 7 days of visible light irradiation.^{14c} The second example, recently reported by our group, is a tetramanganese-containing POM, $[\text{Mn}_4(\text{H}_2\text{O})_2(\text{VW}_9\text{O}_{34})_2]^{10-}$ (Mn_4V_2) that catalyzes hydrogen evolution from water with a TON of 42 after 5.5 h of visible light irradiation. Although the efficiency of the Mn_4V_2 system is higher than that of the Ir^{III}-photosensitized POM catalyst,^{14c} there is still much room for improvement. In an effort to develop more viable (fast, selective and stable), more efficient, and noble-metal-free molecular WRCs, we report here a tetra-nickel-substituted polyoxometalate, $[\text{Ni}_4(\text{H}_2\text{O})_2(\text{PW}_9\text{O}_{34})_2]^{10-}$ (Ni_4P_2), that works as an efficient and robust molecular catalyst for H_2 production in a three-component system upon visible light irradiation.

Ni_4P_2 (Figure 1) was prepared from salts of earth-abundant elements (nickel acetate, sodium tungstate, and Na_2HPO_4) following a modification of the procedure by Coronado, Galán-Mascaros and co-workers¹⁵ and systematically characterized by thermogravimetric analysis, FT-IR, elemental analysis, ESI mass spectrometry, cyclic voltammetry, DFT calculations, and single-crystal X-ray diffraction (see Supporting Information (SI)).

Received: August 16, 2014

Published: September 22, 2014

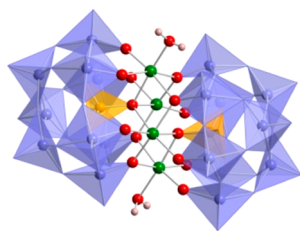


Figure 1. Polyhedral and ball-and-stick representation of Ni_4P_2 . Green, Ni; red, oxygen; pink, H; light blue, WO_6 ; orange, PO_4 .

The visible-light-driven catalytic activity of Ni_4P_2 for hydrogen evolution was examined using a three-component system: $[\text{Ir}(\text{ppy})_2(\text{dtbbpy})]^+$ as photosensitizer, triethanolamine (TEOA) as sacrificial electron donor, and Ni_4P_2 as a WRC. We chose the iridium photosensitizer, $[\text{Ir}(\text{ppy})_2(\text{dtbbpy})]^+$, rather than $[\text{Ru}(\text{bpy})_3]^{2+}$ used in our recent work,^{14d} because its excited state provides more driving force ($[\text{Ir}(\text{ppy})_2(\text{dtbbpy})]^{2+/*} \sim -0.96$ V vs SCE; $[\text{Ir}(\text{ppy})_2(\text{dtbbpy})]^{+/0} \sim -1.51$ V vs SCE in CH_3CN) for successive reduction of the Ni_4P_2 catalyst.¹⁶ Photolysis of a solution of 0.2 mM $[\text{Ir}(\text{ppy})_2(\text{dtbbpy})]^+$, 0.25 M TEOA and catalyst Ni_4P_2 in deaerated $\text{CH}_3\text{CN}/\text{DMF}$ (1/3) using a blue-light-emitting diode (LED) ($\lambda = 455$ nm, 20 mW) at 25 °C results in the reduction of Ni_4P_2 (change in solution color from yellow to green; Figure S9) in agreement with DFT calculations (see SI) and the production of hydrogen. No such color change is observed in the absence of Ni_4P_2 . H_2 production increases linearly with time after exposure to the 455 nm visible light (Figure 2, Figure S10), and no H_2 forms in the dark. A TON of ~ 290 (~ 11.6 μmol H_2 gas per 0.04 μmol catalyst Ni_4P_2) is obtained after 2.5 h of irradiation. This is more than 20 times higher than the Mn_4V_2 WRC.^{14d} Control experiments revealed that all 3 components, i.e., the catalyst Ni_4P_2 , TEOA and $[\text{Ir}(\text{ppy})_2(\text{dtbbpy})]^+$ are essential for efficient H_2 evolution; the absence of any one of these species results in little or no H_2 (Figure S10). An additional control experiment using $\text{TBA}_6[\text{P}_2\text{W}_{18}\text{O}_{62}]$ ($\text{TBA-P}_2\text{W}_{18}$) in place of Ni_4P_2 gives very little H_2 (TON = 1; Figure S10). A Ni^{2+} salt (e.g., NiCl_2), a potential dissociation product of Ni_4P_2 , under otherwise identical conditions gives much less H_2 (Figure S10).

Figure 2 illustrates the reusability of the Ni_4P_2 and NiCl_2 catalysts. The Ni_4P_2 -catalyzed system shows much higher H_2 evolution rates and final yields. A slight decrease of H_2 yield is observed in three successive runs. However, the addition of fresh $[\text{Ir}(\text{ppy})_2(\text{dtbbpy})]^+$ stock solution (0.1 mL of 0.8 mM) fully restores the H_2 evolution activity. The kinetics of H_2 production in the NiCl_2 -catalyzed system shows quickly diminishing yields of H_2 with time. After 12 h of irradiation, the total TON is 1100 and 110 for Ni_4P_2 and NiCl_2 , respectively. Centrifugation of the NiCl_2 -containing solution almost completely removes its photocatalytic activity, indicating the heterogeneity of the system (Figure 2a, red line, pink arrow). This phenomenon is not seen in the Ni_4P_2 -catalyzed system. A scale-up experiment was used to evaluate the long-term robustness of the Ni_4P_2 -catalyzed system. Figure 2b shows that Ni_4P_2 catalyzes H_2 production over 1 week, reaching a TON of 6500 (corresponding to 260 μmol H_2 per 0.04 μmol Ni_4P_2), with little or no loss of catalytic activity, which is, to our knowledge, the highest value for a noble-metal-free POM-catalyzed H_2 evolution system.

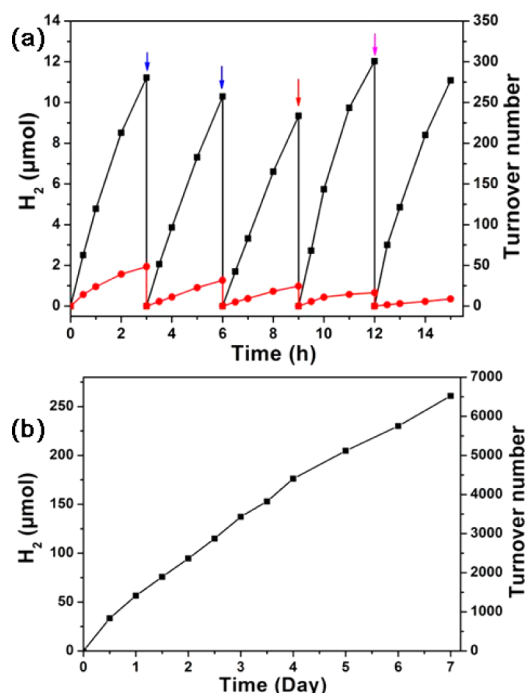


Figure 2. (a) Photocatalytic H_2 evolution using 20 μM Ni_4P_2 (black curve) and 20 μM NiCl_2 (red curve). Conditions: LED light (20 mW, 455 nm), $[\text{Ir}(\text{ppy})_2(\text{dtbbpy})]^+$ (0.2 mM), TEOA (0.25 M), 2 mL $\text{CH}_3\text{CN}/\text{DMF}$ (1/3) deaerated with Ar. (b) Long-term photocatalytic H_2 evolution using Ni_4P_2 (10 μM). Conditions: LED light (20 mW, 455 nm), $[\text{Ir}(\text{ppy})_2(\text{dtbbpy})]^+$ (0.2 mM), TEOA (0.25 M), H_2O (1.4 M), 4 mL $\text{CH}_3\text{CN}/\text{DMF}$ (1/3) deaerated with Ar. Note: the blue arrow means the reaction solution was degassed; the red arrow indicates 0.1 mL of dye (0.8 mM) was added; the pink arrow represents the reaction was centrifuged.

The rate of H_2 evolution depends on the concentrations of catalyst Ni_4P_2 , $[\text{Ir}(\text{ppy})_2(\text{dtbbpy})]^+$ photosensitizer and TEOA sacrificial donor. At constant concentration of $[\text{Ir}(\text{ppy})_2(\text{dtbbpy})]^+$ and TEOA, increasing $[\text{Ni}_4\text{P}_2]$ from 4 to 30 μM results in an increase in the H_2 yield from 1.33 to 15.5 μmol after 2.5 h of irradiation (Figure S11). Figure S13 gives dependences of the rate and final yield of H_2 on the photosensitizer concentration. The amount of H_2 generated increases from 8.5 to 14.1 μmol (corresponding to a TON of ~ 210 to 350, respectively) when varying the $[\text{Ir}(\text{ppy})_2(\text{dtbbpy})]^+$ concentration from 0.1 mM to 0.4 mM. The H_2 yield increases as $[\text{TEOA}]$ increases from 0.05 to 0.25 M (TON increases from 160 to 290; Figure S12).

In photodriven catalytic systems, the photosensitizer excited state can function as either an oxidant or reductant, and thus can be quenched by an electron donor or an acceptor.^{5d,14d,16b,17} To assess the quenching mechanism of our system, the luminescence of the excited photosensitizer, $[\text{Ir}(\text{ppy})_2(\text{dtbbpy})]^{+*}$, in deaerated $\text{CH}_3\text{CN}/\text{DMF}$ (1/3) was measured as a function of both TEOA and separately, Ni_4P_2 concentration (Figure 3a). The linear fitting of a Stern–Volmer plot gives an apparent rate constant of $2.7 \times 10^{10} \text{ M}^{-1} \text{ s}^{-1}$ for oxidative quenching by Ni_4P_2 (Figure S14). The Stern–Volmer analysis of the reductive quenching by TEOA yields a quenching rate constant of $3.3 \times 10^7 \text{ M}^{-1} \text{ s}^{-1}$ (Figure 3b and Figure S14). Although the rate constant for oxidative quenching is about 3 orders of magnitude higher than that of reductive quenching, the reductive process is still dominant

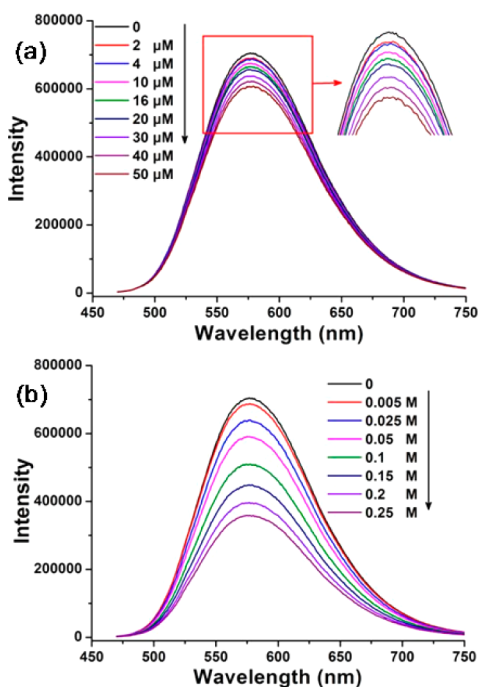


Figure 3. Emission spectra of $[\text{Ir}(\text{ppy})_2(\text{dtbbpy})]^+$ (0.2 mM) as a function of added (a) Ni_4P_2 and (b) TEOA.

given the much higher concentration of TEOA (0.25 M) relative to Ni_4P_2 (20 μM).

To further investigate the electron-transfer steps, time-resolved fluorescence spectroscopy was used to follow the $[\text{Ir}(\text{ppy})_2(\text{dtbbpy})]^{*+}$ luminescence decay kinetics. Figure S15 shows that both Ni_4P_2 and TEOA can accelerate the $[\text{Ir}(\text{ppy})_2(\text{dtbbpy})]^{*+}$ luminescence decay. Single exponential fitting of these kinetics in the presence of Ni_4P_2 and TEOA gives lifetimes of ~ 96 and ~ 52 ns, respectively; however, in the absence of quenchers, the luminescence decay kinetics slow down (lifetime = 103 ns). These data further confirm that catalyst Ni_4P_2 and TEOA can oxidatively and reductively quench the excited state of $[\text{Ir}(\text{ppy})_2(\text{dtbbpy})]^{*+}$ and that the reductive quenching pathway is dominant in agreement with the steady state luminescence quenching results. Transient absorption measurements have also been used to determine the rates of electron-transfer processes. The decay kinetics of $[\text{Ir}(\text{ppy})_2(\text{dtbbpy})]^{*+}$ only is single-exponential with lifetime of ~ 115 ns (Figure S16a and Table S3). In contrast, the lifetime of $[\text{Ir}(\text{ppy})_2(\text{dtbbpy})]^{*+}$ shortens to ~ 98 ns through oxidative quenching by Ni_4P_2 (Figure S16b, Table S3). In addition, $[\text{Ir}(\text{ppy})_2(\text{dtbbpy})]^{*+}$ is also reductively quenched by TEOA with the lifetime of ~ 78 ns (Figure S16c, Table S3), resulting in the formation of one-electron-reduced dye ($\lambda_{\text{max}} = 500$ nm) that further reduces catalyst Ni_4P_2 (Figure S16d, red dash-line circle). On the basis of the above experimental data, we propose the mechanism in Scheme S1 for this visible-light-induced photocatalytic H_2 evolution.

The stability of molecular WRCs under turnover conditions is a general concern. In this context, the photostability of Ni_4P_2 in our system has been examined using multiple physicochemical methods. First, under nonturnover conditions, the UV-vis spectrum of Ni_4P_2 shows no significant change after 24 h (Figure S17). Second, the FT-IR spectra of Ni_4P_2 isolated from postreaction solution after 2.5 h or 7 days remain unchanged relative to the spectrum before photocatalytic reaction (Figure

S18). Third, no decrease of photocatalytic activity by Ni_4P_2 is observed in a mercury-poison test (using up to 150 mg Hg). Fourth, no detectable formation of nanoparticles is observed by either DLS or TEM in the Ni_4P_2 -catalyzed postreaction solution. In contrast, nanoparticles with hydrodynamic sizes centered at 1.5 and 220 nm are observed by DLS in NiCl_2 -catalyzed reactions (Figure S19), consistent with the size distribution (centered at around 2 nm) shown in TEM image (Figure S20). Elemental mapping of these nanoparticles show the presence of both Ni and O, where the O might come from surface oxidation of the Ni nanoparticles upon exposure to air (Figure S20).

In conclusion, we report an efficient, robust, and noble-metal-free molecular POM-based WRC, Ni_4P_2 , that catalyzes H_2 production upon visible-light irradiation over 1 week. It achieves the highest TON value (~ 6500) for a POM-catalyzed H_2 evolution system with no significant loss in activity.

■ ASSOCIATED CONTENT

📄 Supporting Information

Experimental details and data. This material is available free of charge via the Internet at <http://pubs.acs.org>.

■ AUTHOR INFORMATION

Corresponding Author

chill@emory.edu

Notes

The authors declare no competing financial interest.

■ ACKNOWLEDGMENTS

We thank the NSF (Grant No. CHE-0911610) for support. The authors gratefully acknowledge NSF MRI-R2 grant (CHE-0958205) and the use of the resources of the Cherry Emerson Center for Scientific Computation, as well as ONR (Grant No. N00014-13-1-0864) for now-concluded catalytic H_2 evolution experiments.

■ REFERENCES

- (1) (a) Meyer, T. J. *Acc. Chem. Res.* **1989**, *22*, 163. (b) Gratzel, M. *Nature* **2001**, *414*, 338. (c) Lewis, N. S.; Nocera, D. G. *Proc. Natl. Acad. Sci. U.S.A.* **2006**, *103*, 15729. (d) Esswein, A. J.; Nocera, D. G. *Chem. Rev.* **2007**, *107*, 4022. (e) Gray, H. B. *Nat. Chem.* **2009**, *1*, 7. (f) Eisenberg, R. *Science* **2009**, *324*, 44. (g) Faunce, T.; Styling, S.; Wasielewski, M. R.; Brudvig, G. W.; Rutherford, A. W.; Messenger, J.; Lee, A. F.; Hill, C. L.; Fontecave, M.; MacFarlane, D. R. *Energy Environ. Sci.* **2013**, *6*, 1074.
- (2) (a) Brown, G. M.; Brunschwig, B. S.; Creutz, C.; Endicott, J. F.; Sutin, N. *J. Am. Chem. Soc.* **1979**, *101*, 1298. (b) DeLaive, P. J.; Sullivan, B. P.; Meyer, T. J.; Whitten, D. G. *J. Am. Chem. Soc.* **1979**, *101*, 4007.
- (3) (a) Streich, D.; Astuti, Y.; Orlandi, M.; Schwartz, L.; Lomoth, R.; Hammarstrom, L.; Ott, S. *Chem.—Eur. J.* **2010**, *16*, 60. (b) Li, X.; Wang, M.; Chen, L.; Wang, X.; Dong, J.; Sun, L. *ChemSusChem* **2012**, *5*, 913. (c) Berggren, G.; Adamska, A.; Lambert, C.; Simmons, T. R.; Esselborn, J.; Atta, M.; Gambarelli, S.; Mousesca, J. M.; Reijerse, E.; Lubitz, W.; Happe, T.; Artero, V.; Fontecave, M. *Nature* **2013**, *499*, 66.
- (4) (a) Fihri, A.; Artero, V.; Razavet, M.; Baffert, C.; Leibl, W.; Fontecave, M. *Angew. Chem., Int. Ed.* **2008**, *47*, 564. (b) Lazarides, T.; McCormick, T.; Du, P.; Luo, G.; Lindley, B.; Eisenberg, R. *J. Am. Chem. Soc.* **2009**, *131*, 9192. (c) McNamara, W. R.; Han, Z.; Alperin, P. J.; Brennessel, W. W.; Holland, P. L.; Eisenberg, R. *J. Am. Chem. Soc.* **2011**, *133*, 15368. (d) Zhang, P.; Jacques, P.-A.; Chavarot-Kerlidou, M.; Wang, M.; Sun, L.; Fontecave, M.; Artero, V. *Inorg. Chem.* **2012**, *51*, 2115. (e) Singh, W. M.; Baine, T.; Kudo, S.; Tian, S.; Ma, X. A. N.; Zhou, H.; DeYonker, N. J.; Pham, T. C.; Bollinger, J. C.; Baker, D. L.;

Yan, B.; Webster, C. E.; Zhao, X. *Angew. Chem., Int. Ed.* **2012**, *51*, 5941. (f) Khnayzer, R. S.; Thoi, V. S.; Nippe, M.; King, A. E.; Jurss, J. W.; El Roz, K. A.; Long, J. R.; Chang, C. J.; Castellano, F. N. *Energy Environ. Sci.* **2014**, *7*, 1477.

(5) (a) Helm, M. L.; Stewart, M. P.; Bullock, R. M.; DuBois, M. R.; DuBois, D. L. *Science* **2011**, *333*, 863. (b) Small, Y. A.; DuBois, D. L.; Fujita, E.; Muckerman, J. T. *Energy Environ. Sci.* **2011**, *4*, 3008. (c) Han, Z.; Qiu, F.; Eisenberg, R.; Holland, P. L.; Krauss, T. D. *Science* **2012**, *338*, 1321. (d) Han, Z.; McNamara, W. R.; Eum, M.-S.; Holland, P. L.; Eisenberg, R. *Angew. Chem., Int. Ed.* **2012**, *51*, 1667. (e) Han, Z.; Shen, L.; Brennessel, W. W.; Holland, P. L.; Eisenberg, R. *J. Am. Chem. Soc.* **2013**, *135*, 14659.

(6) (a) Karunadasa, H. I.; Chang, C. J.; Long, J. R. *Nature* **2010**, *464*, 1329. (b) Karunadasa, H. I.; Montalvo, E.; Sun, Y.; Majda, M.; Long, J. R.; Chang, C. J. *Science* **2012**, *335*, 698.

(7) (a) Hawecker, J.; Lehn, J. M.; Ziessel, R. *Nouv. J. Chim.* **1983**, *7*, 271. (b) Collin, J. P.; Sauvage, J. P. *Coord. Chem. Rev.* **1989**, *93*, 245. (c) McCormick, T. M.; Han, Z.; Weinberg, D. J.; Brennessel, W. W.; Holland, P. L.; Eisenberg, R. *Inorg. Chem.* **2011**, *50*, 10660.

(8) (a) Hill, C. L. *Chem. Rev.* **1998**, *98*, 1. (b) Hiskia, A.; Mylonas, A.; Papaconstantinou, E. *Chem. Soc. Rev.* **2001**, *30*, 62. (c) Lv, H.; Geletii, Y. V.; Zhao, C.; Vickers, J. W.; Zhu, G.; Luo, Z.; Song, J.; Lian, T.; Musaev, D. G.; Hill, C. L. *Chem. Soc. Rev.* **2012**, *41*, 7572. (d) Cronin, L.; Muller, A. *Chem. Soc. Rev.* **2012**, *41*, 7333. (e) Sumliner, J. M.; Lv, H.; Fielden, J.; Geletii, Y. V.; Hill, C. L. *Eur. J. Inorg. Chem.* **2014**, *2014*, 635.

(9) (a) Geletii, Y. V.; Botar, B.; Kögerler, P.; Hillesheim, D. A.; Musaev, D. G.; Hill, C. L. *Angew. Chem., Int. Ed.* **2008**, *47*, 3896. (b) Sartorel, A.; Carraro, M.; Scorrano, G.; Zorzi, R. D.; Geremia, S.; McDaniel, N. D.; Bernhard, S.; Bonchio, M. *J. Am. Chem. Soc.* **2008**, *130*, 5006. (c) Yin, Q.; Tan, J. M.; Besson, C.; Geletii, Y. V.; Musaev, D. G.; Kuznetsov, A. E.; Luo, Z.; Hardcastle, K. I.; Hill, C. L. *Science* **2010**, *328*, 342. (d) Murakami, M.; Hong, D.; Suenobu, T.; Yamaguchi, S.; Ogura, T.; Fukuzumi, S. *J. Am. Chem. Soc.* **2011**, *133*, 11605. (e) Vickers, J.; Lv, H.; Zhuk, P. F.; Geletii, Y. V.; Hill, C. L. *MRS Proc.* **2012**, *1387*, mrsf11-1387-e02-01. (f) Goberna-Ferrón, S.; Vigara, L.; Soriano-López, J.; Galán-Mascarós, J. R. *Inorg. Chem.* **2012**, *51*, 11707. (g) Stracke, J. J.; Finke, R. G. *ACS Catal.* **2013**, *4*, 79. (h) Schiwon, R.; Klingan, K.; Dau, H.; Limberg, C. *Chem. Commun.* **2014**, *50*, 100.

(10) (a) Geletii, Y. V.; Huang, Z.; Hou, Y.; Musaev, D. G.; Lian, T.; Hill, C. L. *J. Am. Chem. Soc.* **2009**, *131*, 7522. (b) Besson, C.; Huang, Z. Q.; Geletii, Y. V.; Lense, S.; Hardcastle, K. I.; Musaev, D. G.; Lian, T. Q.; Proust, A.; Hill, C. L. *Chem. Commun.* **2010**, *46*, 2784. (c) Huang, Z.; Luo, Z.; Geletii, Y. V.; Vickers, J. W.; Yin, Q.; Wu, D.; Hou, Y.; Ding, Y.; Song, J.; Musaev, D. G.; Hill, C. L.; Lian, T. *J. Am. Chem. Soc.* **2011**, *133*, 2068. (d) Car, P.-E.; Guttentag, M.; Baldrige, K. K.; Alberto, R.; Patzke, G. R. *Green Chem.* **2012**, *14*, 1680. (e) Tanaka, S.; Annaka, M.; Sakai, K. *Chem. Commun.* **2012**, *48*, 1653. (f) Zhu, G.; Glass, E. N.; Zhao, C.; Lv, H.; Vickers, J. W.; Geletii, Y. V.; Musaev, D. G.; Song, J.; Hill, C. L. *Dalton Trans.* **2012**, *41*, 13043. (g) Vickers, J. W.; Lv, H.; Sumliner, J. M.; Zhu, G.; Luo, Z.; Musaev, D. G.; Geletii, Y. V.; Hill, C. L. *J. Am. Chem. Soc.* **2013**, *135*, 14110. (h) Song, F.; Ding, Y.; Ma, B.; Wang, C.; Wang, Q.; Du, X.; Fu, S.; Song, J. *Energy Environ. Sci.* **2013**, *6*, 1170. (i) Lv, H.; Song, J.; Geletii, Y. V.; Vickers, J. W.; Sumliner, J. M.; Musaev, D. G.; Kögerler, P.; Zhuk, P. F.; Bacsa, J.; Zhu, G.; Hill, C. L. *J. Am. Chem. Soc.* **2014**, *136*, 9268. (j) Vickers, J. W.; Sumliner, J. M.; Lv, H.; Morris, M.; Geletii, Y. V.; Hill, C. L. *Phys. Chem. Chem. Phys.* **2014**, *16*, 11942. (k) Han, X.-B.; Zhang, Z.-M.; Zhang, T.; Li, Y.-G.; Lin, W.; You, W.; Su, Z.-M.; Wang, E.-B. *J. Am. Chem. Soc.* **2014**, *136*, 5359.

(11) (a) Toma, F. M.; Sartorel, A.; Iurlo, M.; Carraro, M.; Parisse, P.; Maccato, C.; Rapino, S.; Gonzalez, B. R.; Amenitsch, H.; Da Ros, T.; Casalis, L.; Goldoni, A.; Marcaccio, M.; Scorrano, G.; Scoles, G.; Paolucci, F.; Prato, M.; Bonchio, M. *Nat. Chem.* **2010**, *2*, 826. (b) Quintana, M.; López, A. M.; Rapino, S.; Toma, F. M.; Iurlo, M.; Carraro, M.; Sartorel, A.; Maccato, C.; Ke, X.; Bittencourt, C.; Da Ros, T.; Van Tendeloo, G.; Marcaccio, M.; Paolucci, F.; Prato, M.; Bonchio, M. *ACS Nano* **2013**, *7*, 811. (c) Soriano-López, J.; Goberna-Ferrón, S.;

Vigara, L.; Carbó, J. J.; Poblet, J. M.; Galán-Mascarós, J. R. *Inorg. Chem.* **2013**, *52*, 4753. (d) Guo, S.-X.; Liu, Y.; Lee, C.-Y.; Bond, A. M.; Zhang, J.; Geletii, Y. V.; Hill, C. L. *Energy Environ. Sci.* **2013**, *6*, 2654. (e) Liu, Y.; Guo, S.-X.; Bond, A. M.; Zhang, J.; Geletii, Y. V.; Hill, C. L. *Inorg. Chem.* **2013**, *52*, 11986.

(12) (a) Papaconstantinou, E.; Pope, M. T. *Inorg. Chem.* **1967**, *6*, 1152. (b) Savinov, E. N.; Saidkhanov, S. S.; Parmon, V. N.; Zamaraev, K. I. *React. Kinet. Catal. Lett.* **1981**, *17*, 407. (c) Ioannidis, A.; Papaconstantinou, E. *Inorg. Chem.* **1985**, *24*, 439. (d) Hill, C. L.; Bouchard, D. A. *J. Am. Chem. Soc.* **1985**, *107*, 5148. (e) Yamase, T.; Cao, X.; Yazaki, S. *J. Mol. Catal. A: Chem.* **2007**, *262*, 119.

(13) (a) Keita, B.; Nadjo, L. *J. Electroanal. Chem. Interfacial Electrochem.* **1987**, *217*, 287. (b) Keita, B.; Kortz, U.; Holzle, L. R. B.; Brown, S.; Nadjo, L. *Langmuir* **2007**, *23*, 9531.

(14) (a) Liu, X.; Li, Y.; Peng, S.; Lu, G.; Li, S. *Int. J. Hydrogen Energy* **2012**, *37*, 12150. (b) Zhang, Z.; Lin, Q.; Zheng, S.-T.; Bu, X.; Feng, P. *Chem. Commun.* **2011**, *47*, 3918. (c) Matt, B.; Fize, J.; Moussa, J.; Amouri, H.; Pereira, A.; Artero, V.; Izzet, G.; Proust, A. *Energy Environ. Sci.* **2013**, *6*, 1504. (d) Lv, H.; Song, J.; Zhu, H.; Geletii, Y. V.; Bacsa, J.; Zhao, C.; Lian, T.; Musaev, D. G.; Hill, C. L. *J. Catal.* **2013**, *307*, 48. (e) Suzuki, K.; Tang, F.; Kikukawa, Y.; Yamaguchi, K.; Mizuno, N. *Chem. Lett.* **2014**, *43*, 1429.

(15) Clemente-Juan, J. M.; Coronado, E.; Galán-Mascarós, J. R.; Gomez-Garcia, C. J. *Inorg. Chem.* **1999**, *38*, 55.

(16) (a) Cline, E. D.; Adamson, S. E.; Bernhard, S. *Inorg. Chem.* **2008**, *47*, 10378. (b) Prier, C. K.; Rankic, D. A.; MacMillan, D. W. C. *Chem. Rev.* **2013**, *113*, 5322.

(17) Sun, H.; Hoffman, M. Z. *J. Phys. Chem.* **1994**, *98*, 11719.